Synthesis and Characterization of New Compounds by Enzymatically Catalysed Diels-Alder Reactions

Zainab Adil Jasim[1], Thaer M. M. Al-Rammahi[1], Zeid Hassan Abood[1]

[1]*Department of Chemistry, College of Science, University of Kerbala, Karbala, Iraq*

KEYWORDS

Diels-Alder, Morus alba Diels-Alderase, Enzymatic reactions, Stereochemistry

ABSTRACT

The Diels-Alder (DA) reaction is one of the important chemical transformations to create the C–C bonds with predicted regio- and stereo-selectivity, which lead to the forming of bulk organic molecules. Despite of the significant efforts in this filed, the control of the stereoselectivity of DA reactions remain so difficult. Despite the significant efforts in this field, controlling of stereoselectivity of DA reactions remains so difficult. The design of the enzymatic DA reactions provides scientists with a huge advantage in increasing the selectivity of DA reaction products. This work aims to apply the friendly environmental method includes the application of the current approach in enzymatic DA reactions by formation the new organic compounds through the enzymatic DA reactions between anthracene derivatives as dines and pyrrole derivatives as dienophiles. All DA reactions were curried out in the inert environment using the nitrogen gas. The prepared compounds were caramelized using various techniques including mass spectroscopy, nuclear magnetic resonance, and Fourier transform infrared. The results showed that all products of DA reactions containing unnatural dienes with endo-configuration, in addition to obtain 53%–94% isolated yields. Consequently, this study provides an efficient method to control the stereochemistry of DA reactions.

1. Introduction

The Diels-Alder (DA) reaction is considered one of the most important implications in synthetic organic chemistry, and it applied to develop new organic compounds. A conjugated diene reacts with a dienophile to form a cyclohexene derivative during the DA reaction. This cycloaddition reaction provides six stereocentres with three chirality centers in one step. Among classic approaches, the DA reaction can be modified into hetero-DA, domino-DA, and dehydro-DA reactions to synthesize natural products (1-3). In the last decades, the enzymes termed Diels-Alderases (DAses) have been used as catalysts for the biosynthesis of myriad natural products. All natural DAses have been shown to perform the intramolecular DA, except MaDA and EupfF, which can perform intermolecular [4+2] cycloaddition reactions in the biosynthetic pathway (4-6). These types of enzymes provide opportunities for regio- and stereoselectivity without needing post-reaction modifications, by-product purification, or costly metal catalysts and ionic liquids (7). In 2021, the Nobel Prize in Chemistry was provided to Benjamin List and David MacMillan for developing a new and ingenious molecule building: organocatalysis. This innovation in molecular construction has led to an improvement in the ability to find less expensive and more environmentally friendly biocatalyst pathways (8). Natural products containing a 9,10-anthracenedione substructure have been studied. Recently, the enzymatically catalyzed DA reaction has been applied to form novel organic compounds from anthracene-9,10-diones derivatives (7-11). This work focuses on the current approach in enzymatic Diels−Alder reactions. The new organic compounds have been synthesized in the presence of Morus alba Diels-Alderase (MaDAase) as a catalyst.

The study aims to form new organic compounds by building up the block molecules thought the enzymatic DA reactions between anthracene derivatives as dines and pyrrole derivatives as dienophiles, as shown in Fig.1.

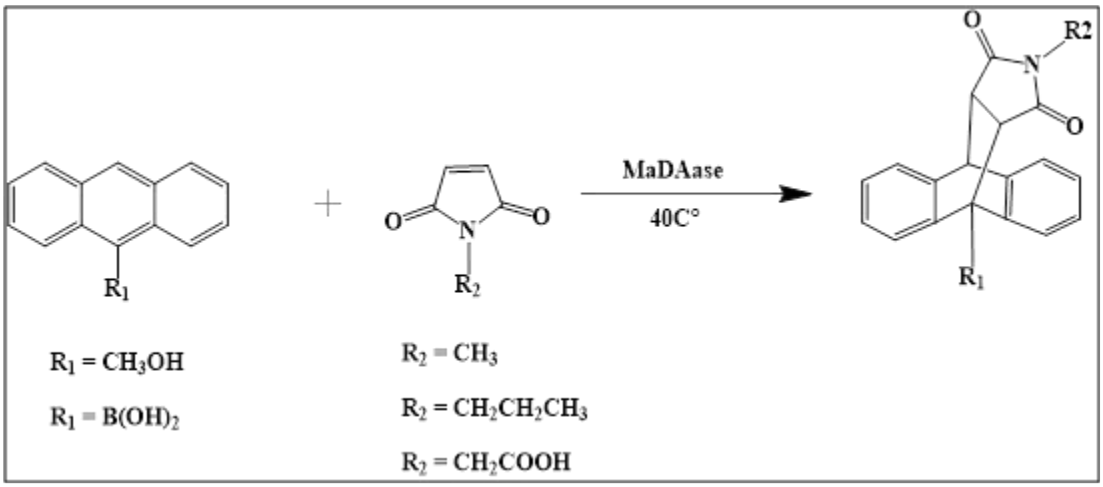

Figure 1. Diels-Alder reactions are catalysed by MaDAase**.**

2. Methodology

This work was conducted at laboratory of postgraduate, Department of Chemistry, College of Science, University of Kerbala, Karbala, Iraq. The mass-spectroscopy measurements were performed using LC-MS Agilent Infinity 1260, in the laboratory of Institution of Science Institute of Organic Chemistry, N.D. Zelinsky Russian Academy of Science, Moscow, Russia. The Nuclear Magnetic Resonance (NMR) were carried out using Avance III 400 MHz NMR spectrometer, in the laboratory of postgraduate, Department of Chemistry, College of Science, University of Basra, Basra, Iraq.

All chemicals include 1-Methyl-1H-pyrrole-2,5-dione (97%), 1-Propyl-1H-pyrrole-2,5-dione (98%), 2-(2,5-Dioxo-2,5-dihydro- 1H-pyrrol-1-yl) acetic acid (97%), 9-Anthraceneboronic acid (98%), 9-Anthracenemethanol (98%) and MaDAase (enzyme activity 1:10) were provided by Hunan Chemfish Pharmaceutical Co., Ltd, Tokyo, Japan.

The solvents include tetrahydrofuran (THF) (99%), absolute ethanol (99%), acetonitrile (97%), deuterated water (D2O) (99%), deuterated dimethyl sulfoxide (DMSO-d6) (99%) and deuterated chloroform (DCl3) (99%) were provided by Sigma-Aldrich, Inc., St. Louis, USA.

All enzymatic DA reactions were performed in an inert environment in the presence of nitrogen gas and completely isolated from the air using the Schlink line technique. The MaDAase enzyme (5 ml, 0.5% w/v) was added into the mixture of anthracene derivative (1 mmol.) and pyrrole derivative in 25 ml tetrahydrofuran (THF). The mixture was reflexed for about 1 hour at 40˚C. The product was filtrated and washed three times using the mixture of deionized water and absolute ethanol (7:3). After that the product dry under vacuum for 2 h, and then recrystallisation and purification using acetonitrile. The physical properties of products for enzymatic DA reactions are presented in Table 1.

Table 1. Physical properties and the yield of DA products

Compound Symbol	Chemical Formula	Mol. wt.	Colour	Melting Point	Yield %
P_1	$C_{20}H_{17}NO_3$	319	Pale yellow	164-166	74
P_2	$C_{22}H_{21}NO_3$	347	Pale yellow	214-216	53
P3	$C_{21}H_{17}NO_5$	363	Pale yellow	145-147	57
P_4	$C_{19}H_{16}BNO_4$	333	Pale yellow	143-145	60
P_5	$C_{21}H_{20}BNO_4$	361	Pale yellow	192-194	70
P_6	$C_{20}H_{16}BNO_6$	377	Pale yellow	194-196	94

3. Result and Discussion

Mass spectroscopy of synthesized compounds

The mass spectrum of P_1 appears signal at (320.1 m/z) relative to the molecular ion, the value close to the calculated molecular weight (319 g/mole), as shown in Fig. 2. The mass spectrum of P_2 appears at (348.3 m/z) relative to the molecular ion, the value close to the calculated molecular weight (347 g/mole), as shown in Fig.3. The mass spectrum of P_3 appears in the signal at (364.1 m/z) relative to the molecular ion, the value close to the calculated molecular weight (363 g/mole), as shown in Fig.4.

Figure 2. Mass spectrum of P_1

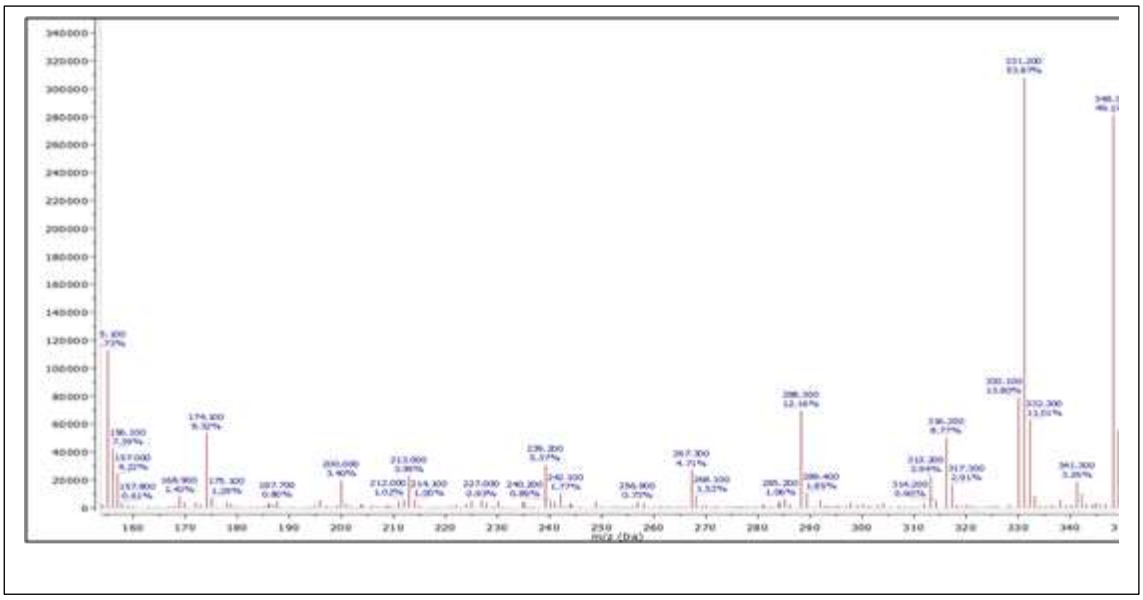

Figure 3. Mass spectrum of P_2

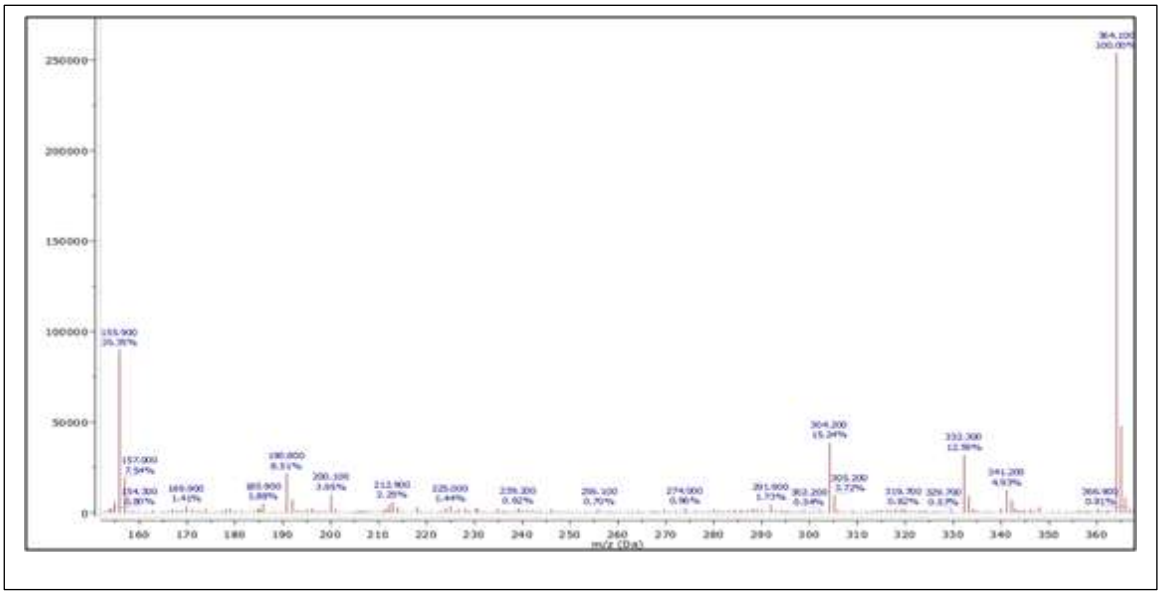

Figure 4. Mass spectrum of P_3.

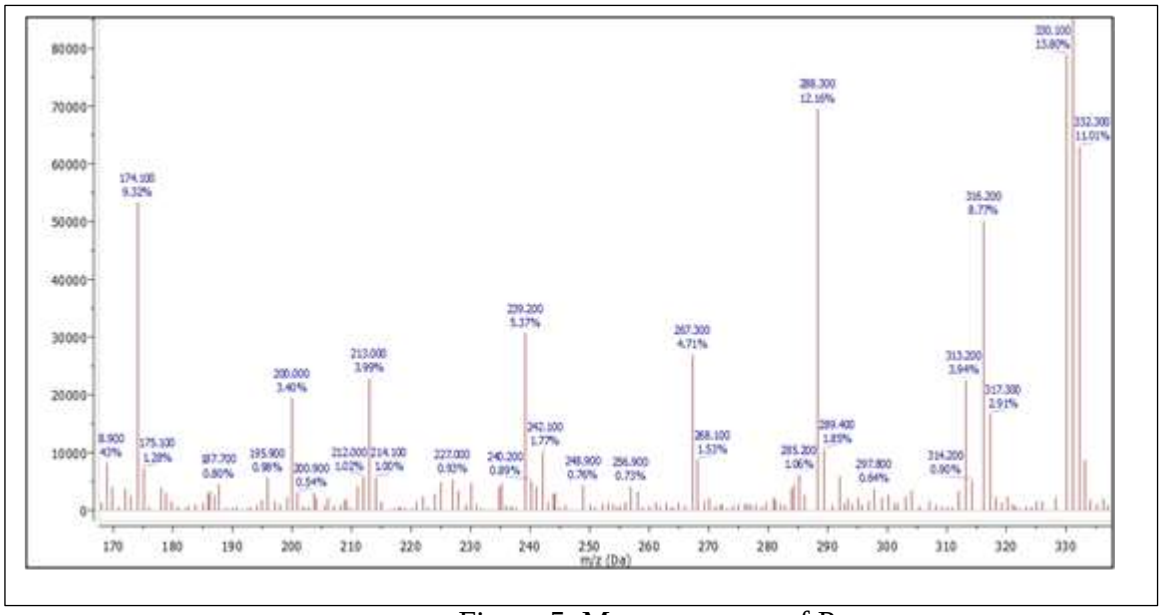

Figure 5. Mass spectrum of P_4.

The mass spectrum of P_4 appears in the signal at (332.9 m/z) relative to the molecular ion, the value close to the calculated molecular weight (333 g/mole), as shown in Fig.5. The mass spectrum of P_5 appears in the signal at (362.1m/z) relative to the molecular ion, the value close to the calculated molecular weight (361 g/mole), as shown in Fig.6. The mass spectrum of P_6 appears in the signal at (378m/z) relative to the molecular ion, the value close to the calculated molecular weight (377 g/mole), as shown in Fig.7.

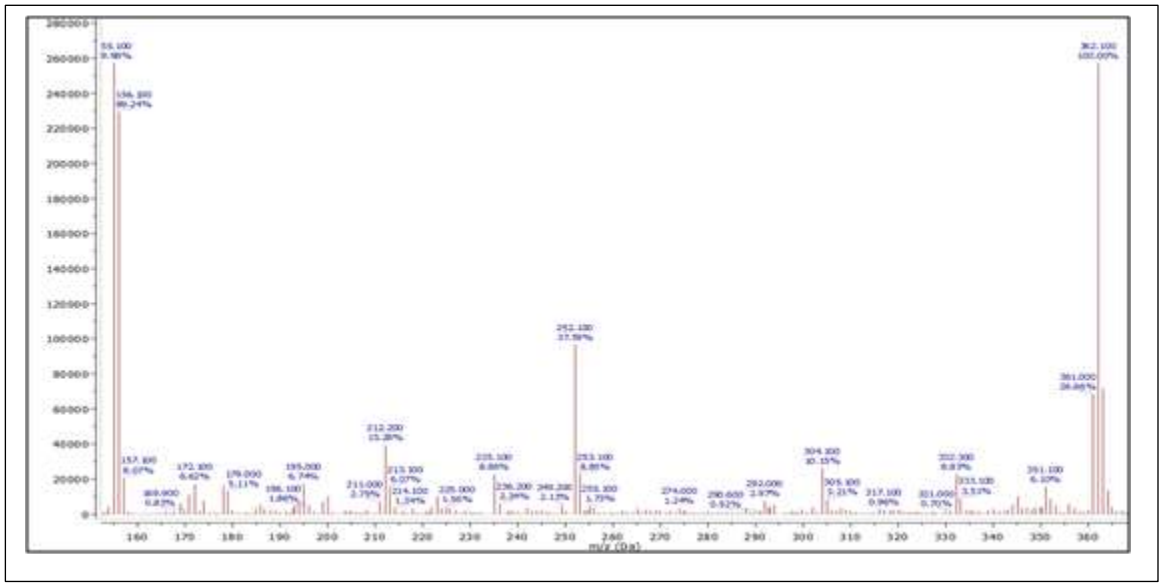

Figure 6. Mass spectrum of P_5.

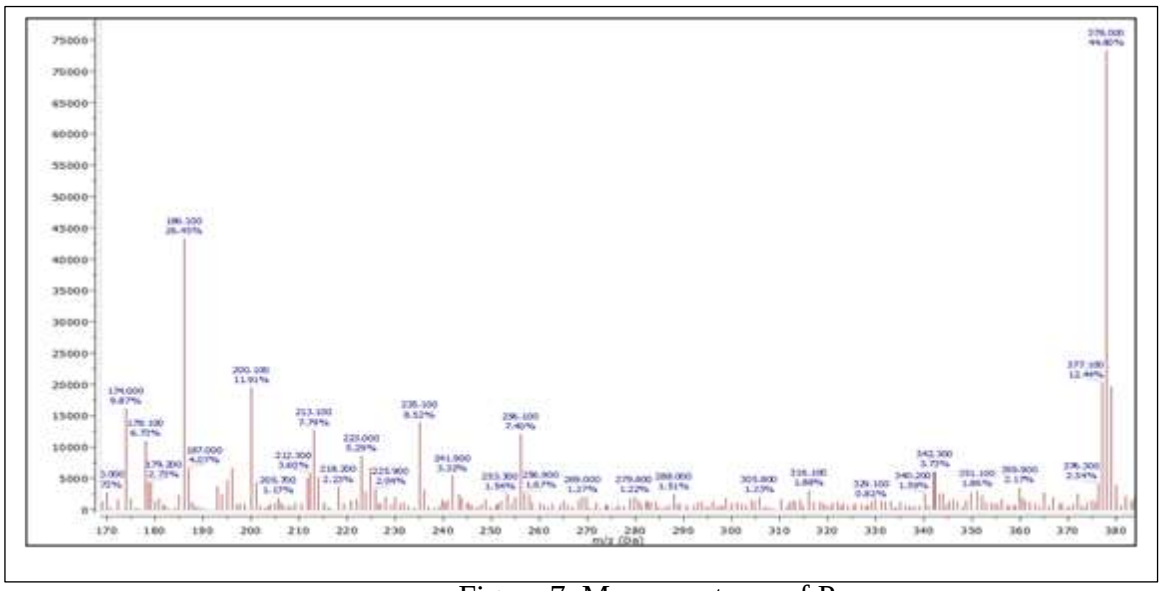

Figure 7. Mass spectrum of P_6.

NMR spectroscopy

^{1}H NMR of synthesized compounds

The ^{1}H NMR spectrum for P_1 in D_2O Fig.8 display the singlet peak at δ (1.32) ppm belong to protons of CH_3 attached to N of pyrrole ring, while the protons of the two CH groups that attached to carbonyl of pyrrole showed multiplet at δ (2.31-2.34) ppm and at δ (2.46-2.50) ppm, respectively. The multiplet peak at δ (3.25-3.29) ppm belong to CH proton of the 9-H anthracene. The signal of (OH) proton of the 10-methyol anthracene appeared the peak at δ (4.68) ppm, in addition to the triplet peak at δ (5.27-5.30) ppm attributed to the protons of CH_2 that attached to hydroxyl group appear. The multiplet peaks at δ (7.09-7.14) ppm, δ (7.21) ppm, δ (7.42-7.44) ppm, and δ (7.65) ppm belong to protons of aromatic rings of anthracene.

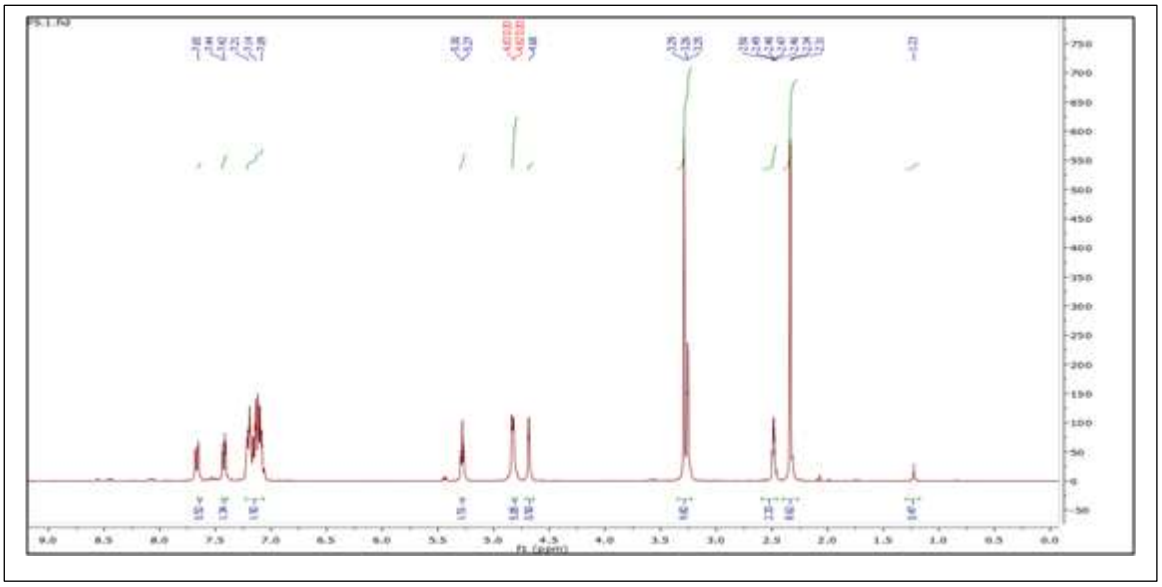

Figure 8. ^{1}H NMR spectrum of P_1

The ^{1}H NMR spectrum for P_2 in D_2O Fig.9 display the quartet peak at δ (0.36-0.41) ppm attributed to the terminal CH_3 of propyl group, which attached with pyrrole, the hexate peak at δ (0.68-0.71) ppm belong to the protons of middle CH_2 of propyl, and the triplet peak at δ (1.2-1.22) belong to the CH_2 of propyl that attached to N of pyrrole ring. The protons of the two CH groups that attached to carbonyl of pyrrole showed multiplet at δ (2.47-2.50) ppm and at δ (2.89-2.93) ppm respectively. The multiplet peak at δ (3.25-3.29) ppm belong to CH proton of the 9-H anthracene. The signal of (OH) proton of the 10-methyol anthracene appeared the peak at δ (4.68) ppm, in addition to the triplet peak at δ (5.30-5.34) ppm attributed to the protons of CH_2 that attached to hydroxyl group. The multiplet peaks at δ (7.11-7.14) ppm, δ (7.41-7.44) ppm, δ (7.64-7.67) ppm, and δ (8.06-8.09) ppm belong to protons of aromatic rings of anthracene.

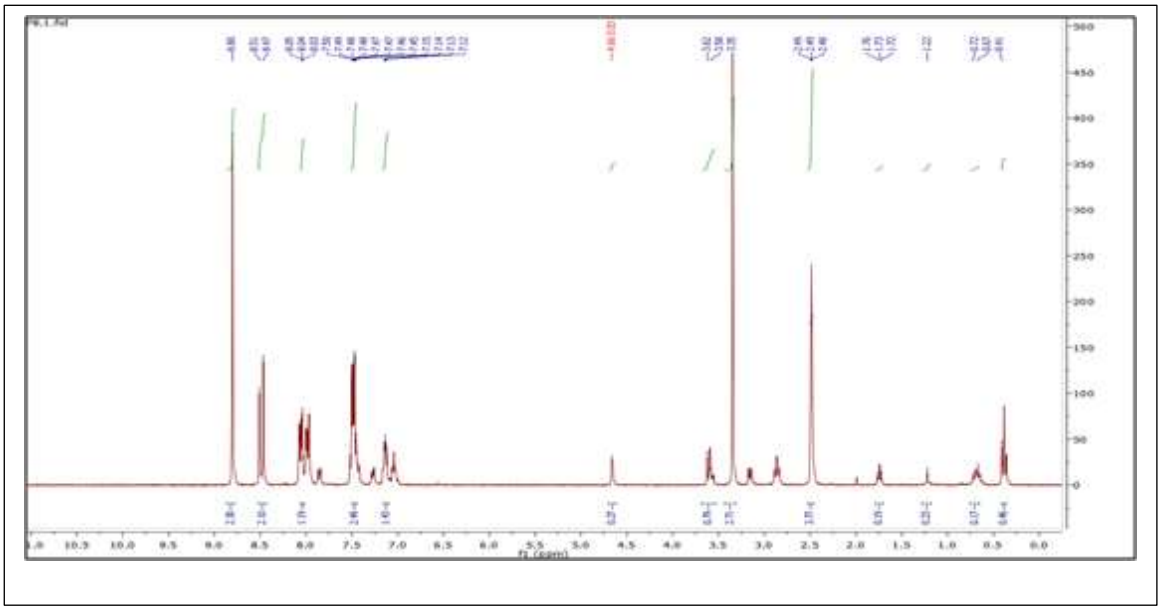

Figure 9. ^{1}H NMR spectrum of P_2

The ^{1}H NMR spectrum for P_3 in D_2O Fig.10 display the singlet peak at δ (1.21) ppm attributed to the CH_2 of acetyl group, which attached with the N of pyrrole. The protons of the two CH groups that attached to carbonyl of pyrrole showed multiplet at δ (2.48-2.50) ppm. The multiplet peak at δ (3.26-3.4) ppm belong to CH proton of the 9-H anthracene. The signal of (OH) proton of the 10-methyol anthracene appeared the peak at δ (4.70) ppm, in addition to the triplet peak at δ (5.35-5.43) ppm

attributed to the protons of CH_2 that attached to hydroxyl group. The signal peak at δ (8.07) ppm attributed to the (OH) of acetyl that attached with pyrrole. The multiplet peaks at δ (7.14-7.18) ppm, δ (7.64-7.66) ppm, and δ (8.43-8.56) ppm belong to protons of aromatic rings of anthracene.

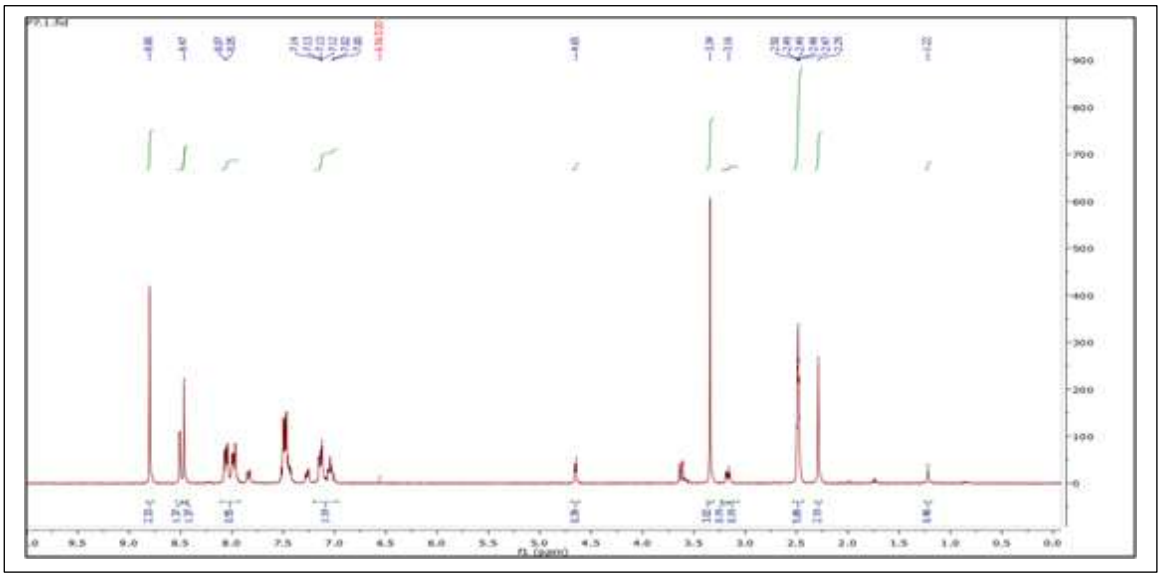

Figure 10. ^{1}H NMR spectrum of P_3

The ^{1}H NMR spectrum for P_4 in D_2O Fig.11 display the singlet peak at δ (1.22) ppm belong to protons of CH_3 attached to N of pyrrole ring, while the protons of the two CH groups that attached to carbonyl of pyrrole showed multiplet at δ (2.29-2.31) ppm and at δ (2.47-2.50) ppm, respectively. The multiplet peak at δ (3.16-3.34) ppm belong to CH proton of the 9-H anthracene. The signal of protons of the two (OH) groups of the 10-boricacid-anthracene appear the peaks at δ (8.47) ppm and δ (8.80) ppm, respectively. The multiplet peaks at δ (7.00-7.02) ppm, δ (7.12-7.14) ppm, and δ (8.05-8.07) ppm belong to protons of aromatic rings of anthracene.

The ^{1}H NMR spectrum for P_5 in D_2O Fig.12 display display the quartet peak at δ (0.41-0.43) ppm attributed to the terminal CH_3 of propyl group, which attached with pyrrole, the hexate peak at δ (0.67-0.72) ppm belong to the protons of middle CH_2 of propyl, and the triplet peak at δ (1.21-1.22) belong to the CH_2 of propyl that attached to N of pyrrole ring. The protons of the two CH groups that attached to carbonyl of pyrrole showed multiplet at δ (1.72-1.76) ppm and at δ (2.48-2.50) ppm, respectively. The multiplet peak at δ (3.35-3.62) ppm belong to CH proton of the 9-H anthracene. The signal of protons of the two (OH) groups of the 10-boricacid-anthracene appear the peaks at δ (8.47) ppm and δ (8.80) ppm, respectively. The multiplet peaks at δ (7.12-7.15) ppm, δ (7.45-7.50) ppm, and δ (8.03-8.08) ppm belong to protons of aromatic rings of anthracene.

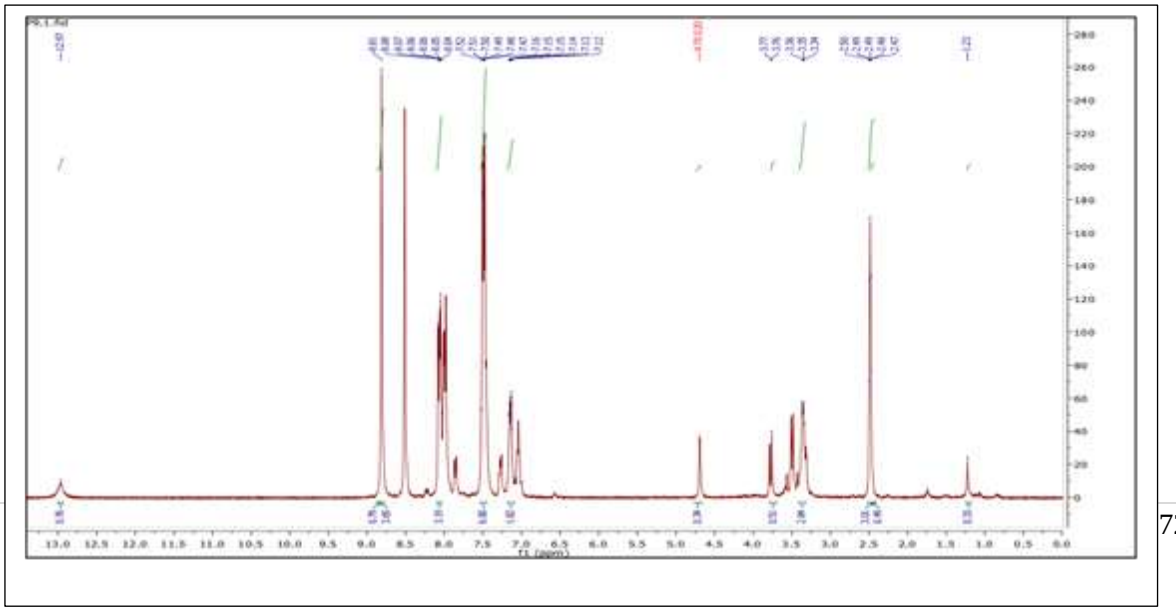

Figure 11. ^{1}H NMR spectrum of P_4

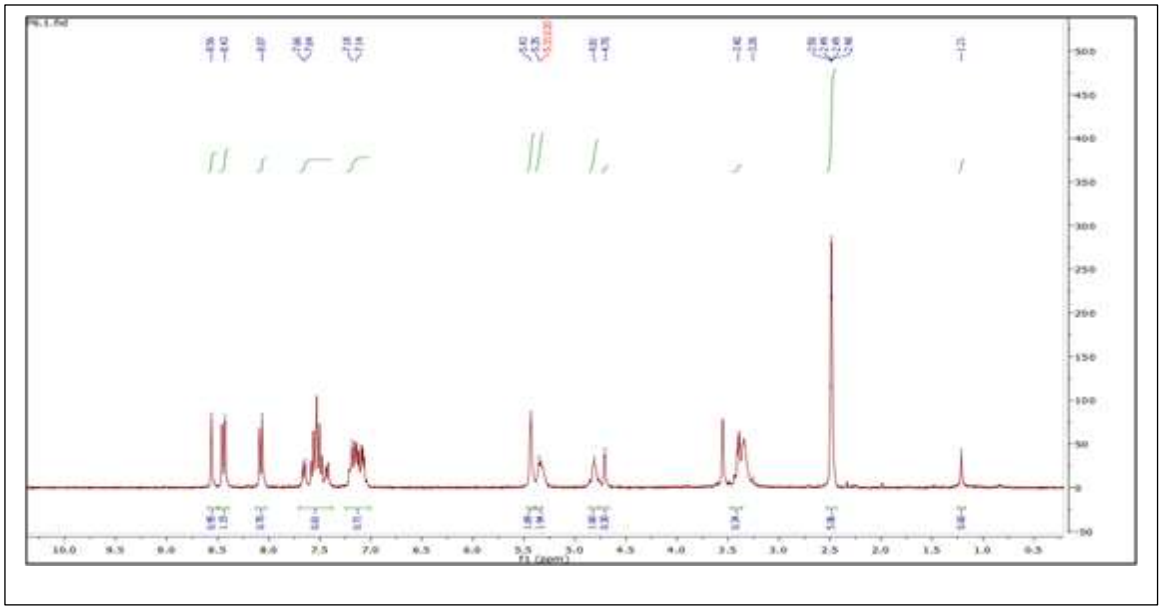

Figure 12. ^{1}H NMR spectrum of P_5

The ^{1}H NMR spectrum for P_6 in D_2O Fig.13 display the singlet peak at δ (1.23) ppm attributed to the CH_2 of acetyl group, which attached with the N of pyrrole. The protons of the two CH groups that attached to carbonyl of pyrrole showed multiplet at δ (2.47-2.50) ppm and at δ (3.34-2.36) ppm, respectively. The multiplet peak at δ (3.76-3.77) ppm belong to CH proton of the 9-H anthracene. The signal of protons of the two (OH) groups of the 10-boricacid-anthracene appear the peak at δ (8.81) ppm. The multiplet peaks at δ (7.12-7.16) ppm, δ (7.47-7.52) ppm, and δ (8.04-8.08) ppm belong to protons of aromatic rings of anthracene. The signal peak at δ (12.97) ppm attributed to the (OH) of acetyl that attached with pyrrole.

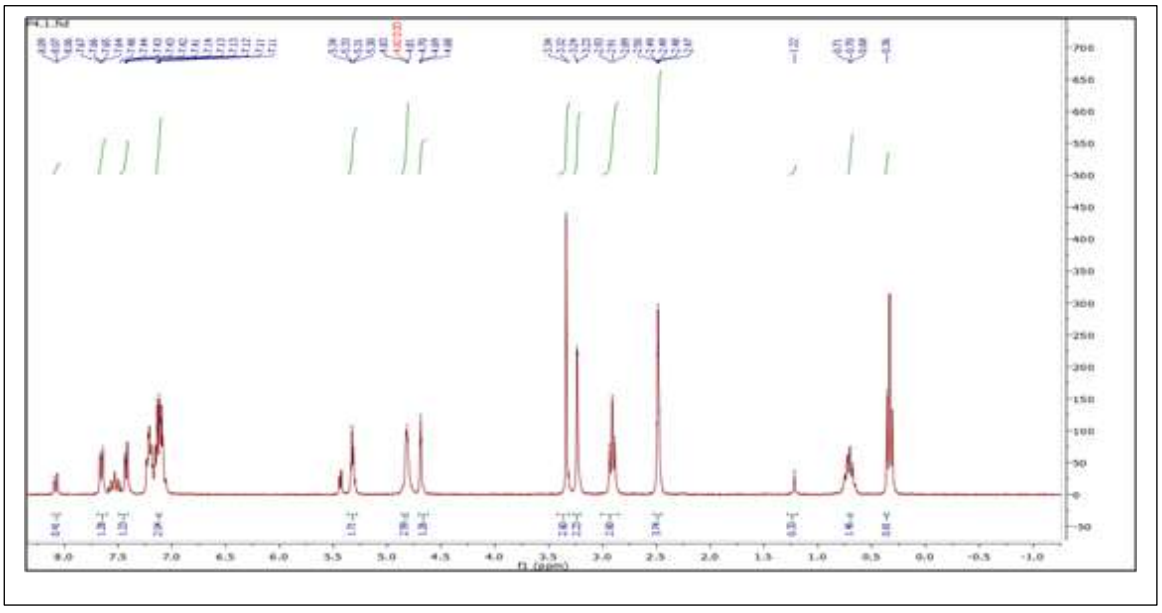

Figure 13. ^{1}H NMR spectrum of P_6

^{13}C NMR of synthesized compounds

The ^{13}C NMR spectrum of P_1 in DMSO-d^6 showed the peak of the carbon atom of methyl group that attaches to N at δ (24.30) ppm. The peak at δ (45.34) ppm belong to the 10-carbon of anthracene that attached to the 10- hydroxymethyl (CH_2-OH) group. The peak at δ (46.06) ppm belong to 9-carbon of anthracene which closed the cycle with pyrrole. The peaks at δ (48.13) ppm and δ (49.67) ppm attributed to the two alpha carbons of pyrrole, respectively. The peak at δ (58.72) ppm belong to carbon of hydroxymethyl that attached to the anthracene. The peaks at δ (122.80) ppm, δ (124.06) ppm, δ (124.82) ppm, δ (125.04) ppm, δ (125.27) ppm, δ (125.50) ppm, δ (126.23) ppm, δ (126.27) ppm, δ (126.57) ppm, δ (126.74) ppm, δ (127.50) ppm, δ (143.05) ppm, and δ (143.10) ppm attributed to the carbons of the anthracene rings. The peaks at δ (176.38) ppm and δ (177.04) ppm attributed to the carbons of the two carbonyl groups for the pyrrole, respectively, Fig.14.

The ^{13}C NMR spectrum of P_2 in DMSO-d^6 showed a peak at δ (11.22) ppm attributed to the terminal CH_3 of propyl that linked with pyrrole, a peak at δ (20.46) ppm attributed to the middle CH_2 of propyl, and a peak at δ (39.56) ppm attributed to the CH_2 of propyl that attached to the N of pyrrole. The peak at δ (45.33) ppm belong to the 10-carbon of anthracene that attached to the 10- hydroxymethyl (CH_2-OH) group. The peak at δ (45.80) ppm belong to 9-carbon of anthracene which closed the cycle with pyrrole. The peaks at δ (47.84) ppm and δ (49.61) ppm attributed to the two alpha carbons of pyrrole, respectively. The peak at δ (58.70) ppm belong to carbon of hydroxymethyl that attached at 10-anthracene. The peaks at δ (124.06) ppm, δ (124.82) ppm, δ (125.53) ppm, δ (126.26) ppm, δ (126.57) ppm, δ (126.73) ppm, δ (127.52) ppm, δ (129.16) ppm, δ (140.49) ppm, and δ (143.21) ppm attributed to the carbons of the anthracene rings. The peaks at δ (176.36) ppm and δ (177.07) ppm attributed to the carbons of the two carbonyl groups for the pyrrole, respectively, see Fig.15.

The ^{13}C NMR spectrum of P_3 in $CDCl_3$ showed the peak at δ (39.10) ppm attributed to the CH_2 of acetyl group, which attached with the N of pyrrole. The peak at δ (39.60) ppm belong to the 10-carbon of anthracene that attached to the 10- hydroxymethyl (CH_2-OH) group. The peaks at δ (45.20) ppm and δ (45.80) ppm attributed to the two alpha carbons of pyrrole, respectively. The peak at δ (55.75) ppm belong to the carbon of hydroxymethyl that attached at 10-anthracene. The peak at δ (58.64) ppm belong to 9-carbon of anthracene which closed the cycle with pyrrole. The peaks at δ (125.14) ppm, δ (125.26) ppm, δ (126.24) ppm, δ (126.71) ppm, δ (129.17) ppm, δ (130.21) ppm, δ (139.73) ppm, δ (140.17) ppm, δ (143.12) ppm, and δ (143.23) ppm attributed to the carbons of the anthracene rings. The peak at δ (168.04) ppm belong to the carbon of the carbonyl for the acetyl that attached to the pyrrole. The peaks at δ (176.36) ppm and δ (177.07) ppm attributed to the carbons of the two carbonyl groups for the pyrrole ring, respectively, see Fig.16.

The ^{13}C NMR spectrum of P_4 in DMSO-d^6 showed the peak of the carbon atom of methyl group that attaches to N at δ (24.24) ppm. The peak at δ (45.84) ppm belong to the 10-carbon of anthracene that attached to the boric acid. The peak at δ (47.80) ppm belong to 9-carbon of anthracene which closed the cycle with pyrrole. The peak at δ (48.51) attributed to the two alpha carbons of pyrrole. The peaks at δ (125.46) ppm, δ (125.60) ppm, δ (125.72) ppm, δ (126.07) ppm, δ (126.37) ppm, δ (127.07) ppm, δ (128.89) ppm, δ (129.50) ppm, δ (131.22) ppm, δ (140.52) ppm, δ (141.78) ppm, δ (143.69) ppm, and δ (144.41) ppm attributed to the carbons of the anthracene rings. The peaks at δ (177.42) ppm and δ (178.25) ppm attributed to the carbons of the two carbonyl groups for the pyrrole ring, respectively, see Fig.17.

The ^{13}C NMR spectrum of P_5 in $CDCl_3$ showed a peak at δ (11.36) ppm attributed to the terminal CH_3 of propyl that linked with pyrrole, a peak at δ (20.40) ppm attributed to the middle CH_2 of propyl, and a peak at δ (39.93) ppm attributed to the CH_2 of propyl that attached to the N of pyrrole. The peak at δ (40.21) ppm belong to the 10-carbon of anthracene that attached to the boric acid. The peak at δ (40.48) ppm belong to 9-carbon of anthracene which closed the cycle with pyrrole. The peak at δ (40.76) ppm attributed to the two alpha carbons of pyrrole ring. The peaks at δ (124.53) ppm, δ (124.88) ppm, δ (125.46) ppm, δ (125.60) ppm, δ (125.72) ppm, δ (126.05) ppm, δ (126.33) ppm, δ (126.38) ppm, δ (127.16) ppm, δ (131.22) ppm, δ (133.18) ppm, δ (140.63) ppm, and δ (143.84) attributed to the carbons of the anthracene rings. The peaks at δ (177.37) ppm and δ (178.23) ppm attributed to the carbons of

the two carbonyl groups for the pyrrole, respectively, see Fig.18.

The ^{13}C NMR spectrum of P_6 in DMSO-d^6 showed the peak at δ (39.19) ppm attributed to the CH_2 of acetyl group, which attached with the N of pyrrole. The peak at δ (41.98) ppm belong to the 10-carbon of anthracene that attached to the boric acid. The peaks at δ (45.80) ppm and δ (47.62) ppm attributed to the two alpha carbons of pyrrole, respectively. The peak at δ (48.41) ppm belong to 9-carbon of anthracene which closed the cycle with pyrrole. The peaks at δ (124.66) ppm, δ (124.83) ppm, δ (125.47) ppm, δ (125.61) ppm, δ (126.20) ppm, δ (126.39) ppm, δ (126.48) ppm, δ (127.15) ppm, δ (128.90) ppm, δ (131.23) ppm, δ (140.35) ppm, and δ (141.63) ppm attributed to the carbons of the anthracene rings. The peak at δ (168.22) ppm belong to the carbon of the carbonyl for the acetyl that attached to the pyrrole. The peaks at δ (176.55) ppm and δ (177.31) ppm attributed to the carbons of the two carbonyl groups for the pyrrole ring, respectively, see Fig.19.

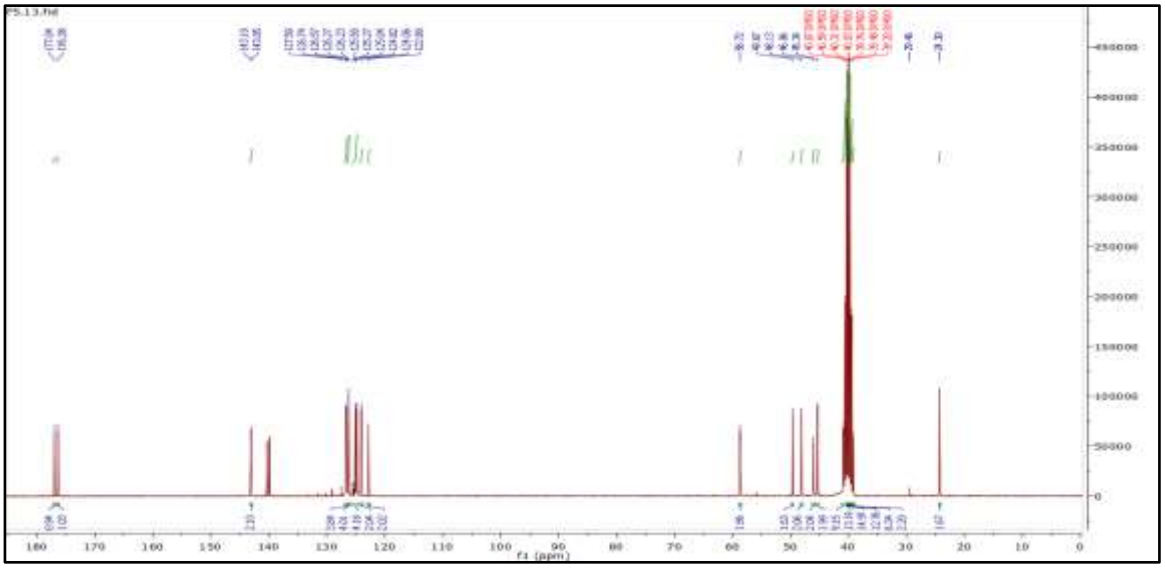

Figure 14. ^{13}C NMR spectrum of P_1

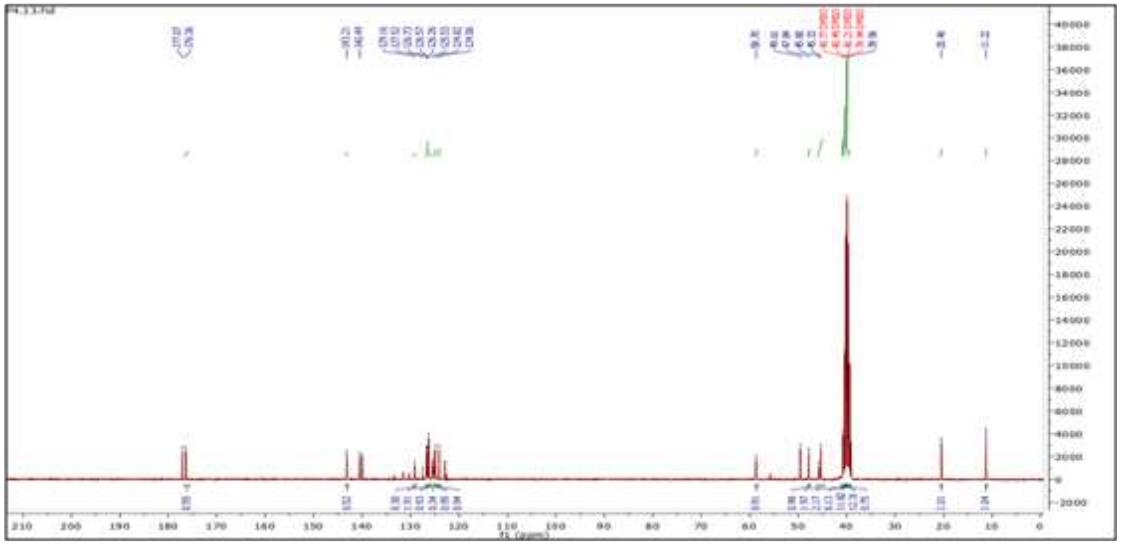

Figure 15. ^{13}C NMR spectrum of P_2

Figure 16. ^{13}C NMR spectrum of P_3

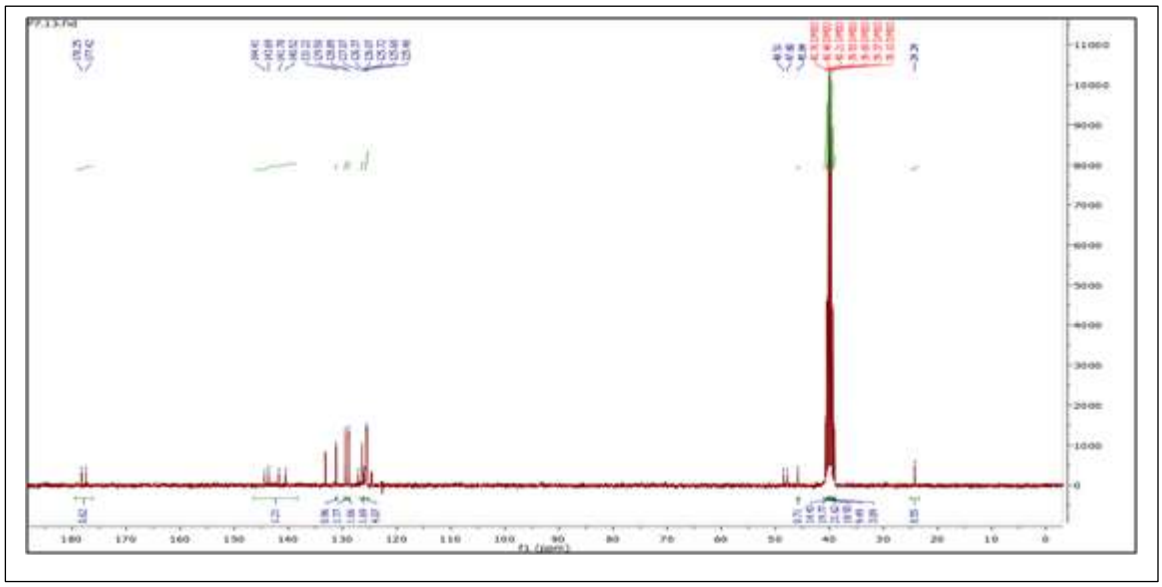

Figure 17. ^{13}C NMR spectrum of P_4

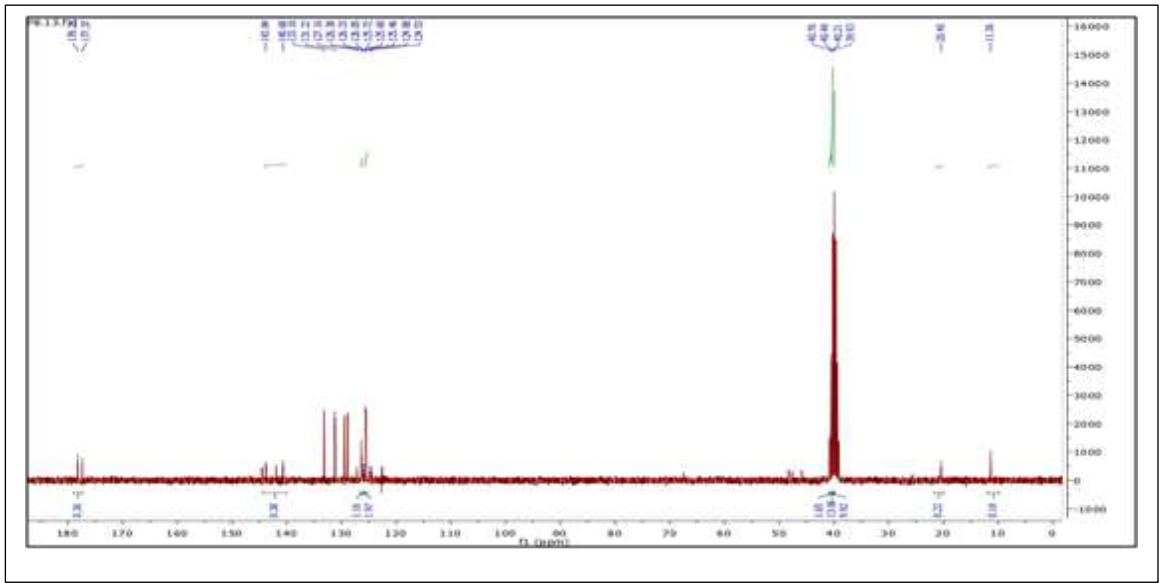

Figure 18. ^{13}C NMR spectrum of P_5

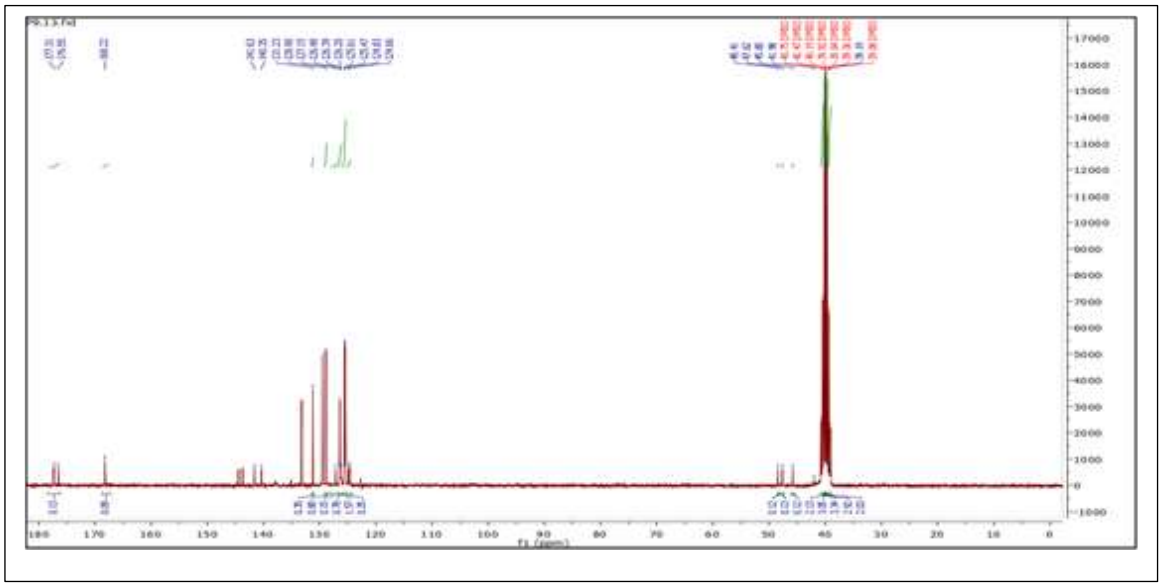

Figure 19. ^{13}C NMR spectrum of P_6.

Fourier transform infrared (FTIR) spectroscopy

The FTIR spectrum of P_1 exhibited a medium broad peak at 3502 cm^{-1} refer to the OH belong to terminal OH of hydroxymethyl that attached at 10-anthracene. The weak peak at 3066 cm^{-1} belong to the stretching C-H (SP^2) for the pyrrole ring. In addition, the two weak peaks at 2958 cm^{-1}, and 2877 cm^{-1} belong to C-H(SP^3) of the methyl, which linked to the pyrrole ring. The two peaks that related to stretching active carbonyl amide groups of pyrrole ring appeared as the weak peak at 1766 cm^{-1} and the strong sharp peak at 1693 cm^{-1}. The medium peak at 1462 cm^{-1} belong to C=C of anthracene rings. The medium peak at 1207 cm^{-1} attributed to the (C-O) bond of alcohol for the hydroxymethyl.

The FTIR spectrum of P_2 showed a medium peak at 3495 cm^{-1} belong to terminal OH of hydroxymethyl that attached at 10-anthracene. The weak peak at 3066 cm^{-1} attributed to the stretching C-H (SP^2) for the pyrrole ring. The weak peaks at 2943 cm^{-1}, 2897 cm^{-1}, and 2839 cm^{-1} belong to C-H (SP^3) of the propyl, which linked to the pyrrole ring. The two stretching peaks related to the active carbonyl for pyrrole ring, appeared as the weak peak at 1766 cm^{-1} and the strong sharp peak at 1689 cm^{-1}. The weak peak at 1546 cm^{-1} belong to C=C of the anthracene rings. The medium peak at 1292 cm^{-1} attributed to the (C-O) bond of alcohol for the hydroxymethyl.

The FTIR spectrum of P_3 showed a medium broad peak at 3417 cm^{-1} belonging to OH for both the acetyl linked to the pyrrole and the terminal OH of hydroxymethyl attached at 10-anthracene. The weak peak at 3093 cm^{-1} refer to the stretching C-H (SP^2) for the pyrrole ring. The weak peaks at 2951 cm^{-1} and 2912 cm^{-1} attributed to C-H (SP^3) of acetyl. The weak peak at 1766 cm^{-1} and the strong peak at 1697 cm^{-1} attributed to the stretching active carbonyl amide of pyrrole. The weak peak at 1516 cm^{-1} belong to C=C of the anthracene rings. The medium peak at 1234 cm^{-1} attributed to the (C-O) bond of alcohol for the hydroxymethyl.

The FTIR spectrum of P_4 exhibited the strong a broad peak at 3333 cm^{-1} and the medium broad peak at 3279 cm^{-1} attributed to the two OH of the boric acid that linked at 10-anthracene. The weak peak at 3074 cm^{-1} belong to the stretching C-H (SP^2) for the pyrrole ring. In addition, the weak peak at 2955 cm^{-1} belong to C-H (SP^3) of the methyl, which linked to the pyrrole ring. The two peaks that related to stretching active carbonyl amide groups of pyrrole ring appeared as the weak peak at 1766 cm^{-1} and the strong sharp peak at 1685 cm^{-1}. The weak peak at 1550 cm^{-1} belong to C=C of anthracene rings.

The FTIR spectrum of P_5 appeared the strong a broad peak at 3329 cm^{-1} attributed to the two OH of the boric acid that linked at 10-anthracene. The weak peak at 3051 cm^{-1} attributed to the stretching C-

H (SP^2) for the pyrrole ring. The weak peaks at 2943 cm^{-1}, 2878 cm^{-1}, and 2885 cm^{-1} belong to C-H (SP^3) of the propyl, which linked to the pyrrole ring. The two stretching peaks related to the active carbonyl for pyrrole ring, appeared as the weak peak at 1763 cm^{-1} and the strong sharp peak at 1681 cm^{-1}. The weak peak at 1554 cm^{-1} belong to C=C of the anthracene rings.

The FTIR spectrum of P_6 showed the strong a broad peak at 3329 cm^{-1} attributed to the two OH of the boric acid that linked at 10-anthracene and the acetyl linked to the pyrrole. The weak peak at 3051 cm^{-1} refer to the stretching C-H (SP^2) for the pyrrole ring. The weak peak at 2958 cm^{-1} attributed to C-H (SP^3) of acetyl. The weak peak at 1734 cm^{-1} and the strong peak at 1693 cm^{-1} attributed to the stretching active carbonyl amide of pyrrole. weak peak at 1620 cm^{-1} belong to the carbonyl of acetyl that linked to the pyrrole ring. The weak peak at 1558 cm^{-1} belong to C=C of the anthracene rings. The medium peak at 1255 cm^{-1} attributed to the carboxylic (C-O) bond of acetyl that attached pyrrole.

Discussion

The study showed that it can be explored whether the peri-selectivity of MaDAase could be switched to favour of the hetero-Diels–Alder reaction. To take advantage of their substrate promiscuity, endo-selective MaDA was used for the chemo-enzymatic synthesis of D-A natural products. All products of DA reactions containing unnatural dienes with endo-configuration were obtained as the main product in 53%–94% isolated yields using MaDA as the catalyst, these findings are analogs to the previous study containing non-natural dienes or/and dienophiles (12). On the other hand, the two different approaches to artificially create intermolecular Diels-Alderases were performed in earlier work (13). Further applications for the genome mining of new Diels-Alderases from microbial natural products provided strong evidence of these biosynthetic pathways to formation of the novel organic compounds (14). Although considerable achievements in this research area, the comparing between intermolecular Diels-Alderases and intramolecular Diels-Alderases in nature still very limited.

In general, this study applies the updated remarkable discoveries of intermolecular Diels-Alderases and provides a future vision of the potential applications of Diels-Alderase in biocatalysis. As a result, efforts are made to discover and implement the biosynthetic pathways to improve the ability to form functional organic molecules more efficiently.

Reference

[1] Sara AA, Saeed A, Kalesse M. Recent Applications of the Diels–Alder Reaction in the Synthesis of Natural Products (2017–2020). Synthesis. 2022; 54(04): 975-998. DOI: 10.1055/a-1532-4763.

[2] Briou B, Améduri B, Boutevin B. Trends in the Diels–Alder reaction in polymer chemistry. Chem. Soc. Rev., 2021,50, 11055-11097. DOI: 10.1039/D0CS01382J.

[3] Mali G, Chauhan AN, Chavan KA, Erande RD. Development and applications of double Diels-Alder reaction in organic synthesis. Asian Journal of Organic Chemistry. 2021 Nov;10(11):2848-68. DOI: 10.1002/ajoc.202100493.

[4] Oikawa, H. Nature's strategy for catalyzing Diels-Alder reaction. Cell Chem. Biol. 23, 429–430 (2016).

[5] Gao, L. et al. FAD-dependent enzyme-catalysed intermolecular [4+2] cycloaddition in natural product biosynthesis. Nat. Chem. 12, 620–628 (2020).

[6] Chen, Q. et al. Enzymatic intermolecular hetero-Diels-Alder reaction in the biosynthesis of tropolonic sesquiterpenes. J. Am. Chem. Soc. 141, 14052–14056 (2019)

[7] Avendaño C, López-Alvarado P, Pérez JM, Alonso MÁ, Pascual-Alfonso E, Ruiz-Serrano M, Menéndez JC. Structure-Antitumor Activity Relationships of Aza-and Diaza-Anthracene-2, 9, 10-Triones and Their Partially Saturated Derivatives. Molecules. 2024 Jan 18;29(2):489. DOI: 10.3390/molecules29020489.

[8] Enzymatic intermolecular Diels-Alder reactions in synthesis: From nature to design, Tetrahedron Chem., (2); 1-11, (2022). DOI: 10.1016/j.tchem.2022.100013.

[9] Sirazhetdinova NS, Savelyev VA, Frolova TS, Baev DS, Klimenko LS, Chernikov IV, Oleshko OS, Sarojan TA, Pokrovskii AG, Shults EE. 1-Hydroxyanthraquinones Containing Aryl Substituents as Potent and Selective Anticancer

Agents. Molecules. 2020 May 29;25(11):2547. DOI: 10.3390/molecules25112547.

[10] Malik MS, Alsantali RI, Jassas RS, Alsimaree AA, Syed R, Alsharif MA, Kalpana K, Morad M, Althagafi II, Ahmed SA. Journey of anthraquinones as anticancer agents–a systematic review of recent literature. RSC advances. 2021;11(57):35806-27. DOI: 10.1039/d1ra05686g.

[11] Kashyap R, Veera Yerra N, Oja J, Bala S et al. Exo-selective intermolecular Diels–Alder reaction by PyrI4 and AbnU on non-natural substrates. Commun Chem. 2021; 4, 113. DOI: 10.1038/s42004-021-00552-9.

[12] Gao, L., Zou, Y., Liu, X. et al. Enzymatic control of endo- and exo-stereoselective Diels–Alder reactions with broad substrate scope. Nat Catal. 2021; 4, 1059–1069. DOI: 10.1038/s41929-021-00717-8.

[13] W. Ghattas, J.-P. Mahy, M. Reglier, A.J. Simaan. Artificial enzymes for Diels-Alder reactions. Chembiochem. 2021; 22, 443-459. DOI: 10.1002/cbic.202000316.

[14] L. Gao, X. Lei. Biosynthetic Intermediate Probes for Visualizing and Identifying the Biosynthetic Enzymes of Plant Metabolites. ChemBioChem. 2021; 22, 982. DOI: 10.1002/cbic.202000530..